

Supplementary Material for Minimal BRDF Sampling for Two-Shot Near-Field Reflectance Acquisition

Zexiang Xu¹ Jannik Boll Nielsen² Jiyang Yu¹ Henrik Wann Jensen¹ Ravi Ramamoorthi^{1*}
¹University of California, San Diego ²Technical University of Denmark

Convergence Plot (Section 5): Figure 1 shows the convergence of the near-field optimization for 50 random initial conditions, with $n = 2$ samples and a 25° field of view. Light and view directions for each run converge to almost the same directions. Similar results hold for other fields of view.

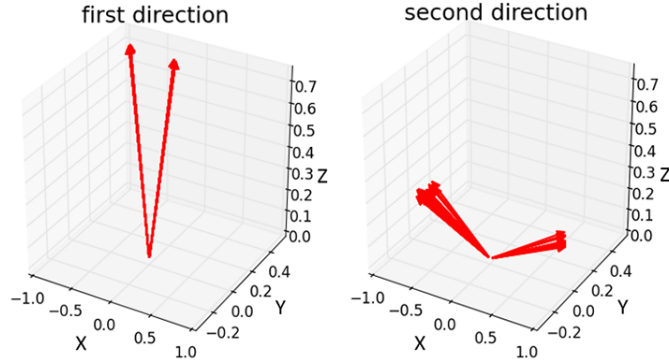


Figure 1: Optimization repeated 50 times for $n = 2$ images for near-field sampling with a 25° field of view. Light and view directions for each run converge to almost the same location.

Larger Fields of View and More Samples (Section 6): Figure 2 extends Fig. 6 in the main paper by also showing average RMS error in reconstruction for two much wider fields of view, of 85° and 175° . It can be seen that there is minimal change in the error curves, even for these extreme field of view angles. This justifies our use of 25° field of view for most of the results in the main paper.

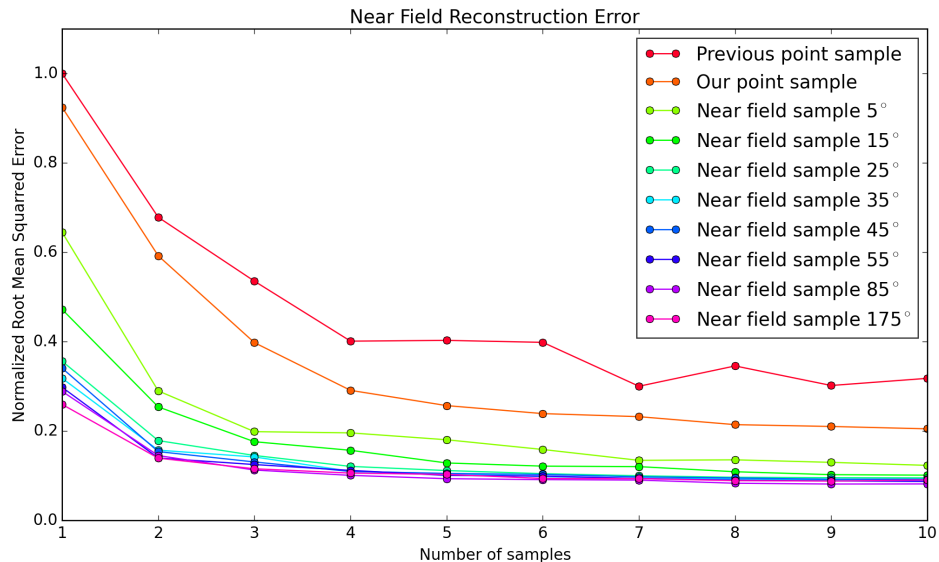


Figure 2: Average RMS error over unknown samples for near-field reflectance acquisition. This extends Fig. 6 in the main paper by adding two wide field-of-view angles of 85° and 175° . As with the main paper, errors are measured in the log-mapped BRDF domain.

*email {zexiangxu, jiy173, henrik, ravir }@eng.ucsd.edu, jbol@dtu.dk

Figure 3 extends Fig. 8 of the main paper, also listing the optimal sampling directions for 3, 4 and 5 near-field images for fields-of-view from 15° to 45° . These directions may be useful for those implementers interested in using even more images than the two-shot acquisition discussed in the main paper.

n	$\theta_h [^\circ]$	$\theta_d [^\circ]$	$\phi_d [^\circ]$
3	0	46	0
	4	80	88
	30	36	38
4	0	16	0
	0	58	0
	4	83	88
	31	34	38
5	0	16	0
	0	58	0
	4	83	88
	24	67	40
	31	30	32

n	$\theta_h [^\circ]$	$\theta_d [^\circ]$	$\phi_d [^\circ]$
3	3	30	36
	15	79	87
	35	39	34
4	2	61	173
	3	28	36
	24	83	88
	35	38	34
5	1	68	0
	3	27	36
	23	70	45
	24	83	88
	31	35	40

n	$\theta_h [^\circ]$	$\theta_d [^\circ]$	$\phi_d [^\circ]$
3	4	39	3
	8	79	82
	34	43	21
4	3	56	4
	8	82	81
	8	12	56
	34	44	27
5	1	76	0
	1	54	0
	6	85	81
	8	12	56
	36	43	36

n	$\theta_h [^\circ]$	$\theta_d [^\circ]$	$\phi_d [^\circ]$
3	1	82	0
	3	56	6
	12	12	89
4	1	82	0
	1	57	0
	10	13	86
	38	50	44
5	1	85	0
	1	76	0
	1	54	0
	10	13	86
	40	44	41

Figure 3: Tabulation of 3, 4 and 5 near-field acquisition directions for fields of view ranging from 15° to 45° .

Point Sampling (Appendix B): Figure 4 lists our optimal point-sampling directions for 1,2,5,10 and 20 samples. Qualitatively, the directions are similar to those in [Nielsen et al. 2015]; for example, the one sample measurement focuses on specular reflection with $\theta_h = 0$. Indeed, we typically use several samples at mirror reflection $\theta_h = 0^\circ$, to precisely measure the specular highlight. However, the actual locations are different from [Nielsen et al. 2015], and produce somewhat more accurate results.

n	$\theta_h [^\circ]$	$\theta_d [^\circ]$	$\phi_d [^\circ]$
1	0	57	0
	0	57	0
2	14	22	167
	0	75	0
5	0	37	0
	3	83	112
	5	50	160
	33	30	138
	0	30	0
10	0	74	0
	1	84	0
	2	64	84
	2	31	43
	9	12	135
	10	81	42
	16	64	71
	38	6	132
	50	52	121
	0	31	0
20	0	85	0
	0	70	0
	0	13	0
	1	59	0
	1	84	0
	2	32	176
	4	75	65
	4	14	54
	8	44	108
	8	73	0
	10	81	42
	14	9	170
	17	15	117
	18	65	66

Figure 4: Optimal light-view sampling directions from our method for point-sampled BRDF measurement.

We compare reconstructions for a few materials from the MERL database for our directions, and for [Nielsen et al. 2015] in Fig. 5. It can be seen that in some cases we do qualitatively better, while there is a minor improvement in other cases. In general, our 5 directions produces comparable results to 20 samples using the previous condition number metric.

Figure 18 in Appendix B of the main paper shows a comparison with [Nielsen et al. 2015] for reconstruction with no noise, as in the original work of [Nielsen et al. 2015]. Figure 6 below extends this, by showing a comparison of reconstruction with our optimized 20 directions and the previous work, assuming a noise β of 0.02. The results are comparable to those in the main paper, with our errors always being lower.

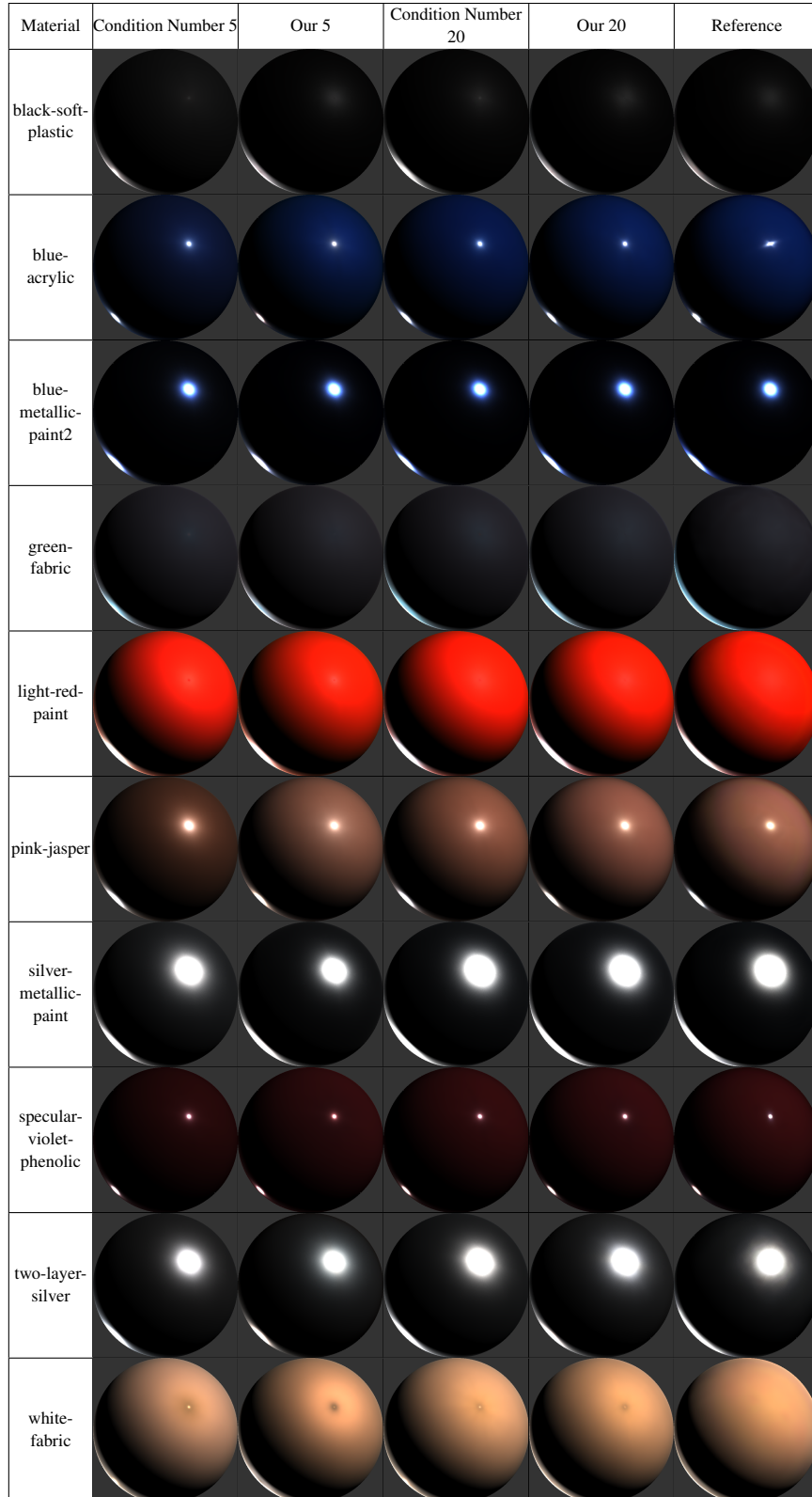


Figure 5: Comparison of MERL BRDF materials reconstructed using our new optimized sampling directions, and those obtained with the sampling directions in [Nielsen et al. 2015]. Our results show a minor improvement, with a qualitative benefit in some cases.

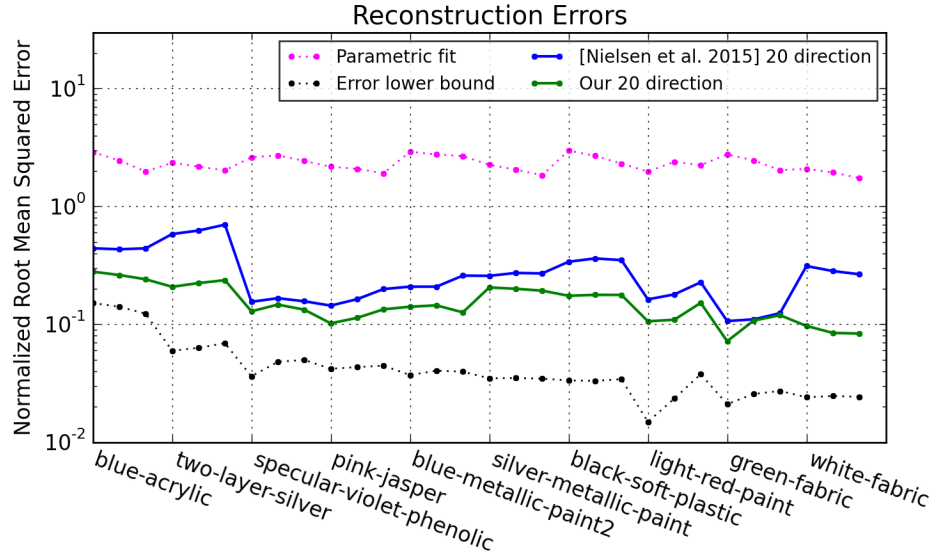
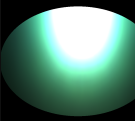
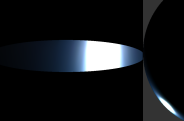
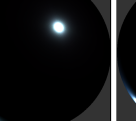
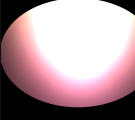
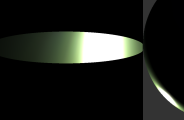
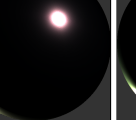
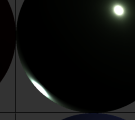
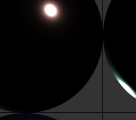
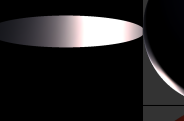
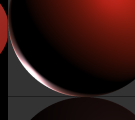
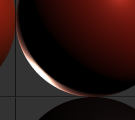
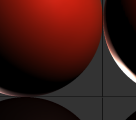
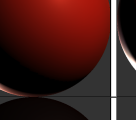
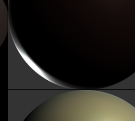
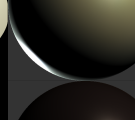
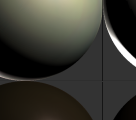
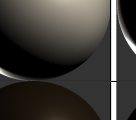
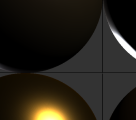
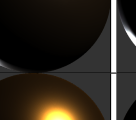
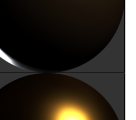
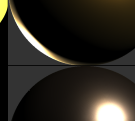
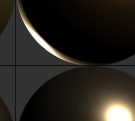
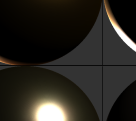
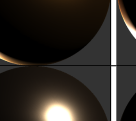
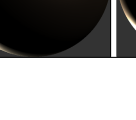


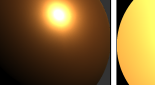
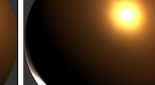
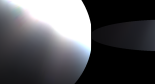
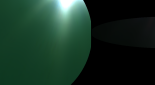
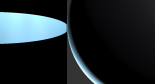
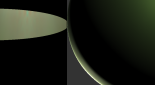
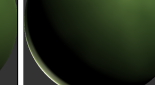
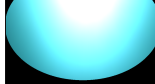
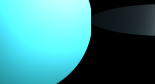
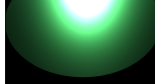
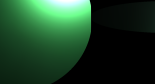
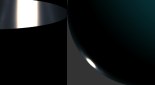
Figure 6: Comparison of reconstruction with our new optimized directions, and those from [Nielsen et al. 2015], where we consider 20 directions instead of 5 in the main paper, and include noise of 2%. Our method again produces a lower error.

Comparison of Near-Field and Point Sampling (Figure 2): The remainder of the document is similar to Fig. 2 of the main paper, showing simulations of the MERL BRDF materials, but for all of the materials in the database using our final optimized set of near-field directions. It can be seen that over the entire database, one image in near-field sampling is similar to 5 point samples and two images in near-field sampling is similar to 20 point samples.

Material	Sample image	Near field 25° 1	Point sample 5	Sample image 1	Sample image 2	Near field 25° 2	Point sample 20	Reference
alum-bronze								
alumina-oxide								
aluminium								
aventurine								
beige-fabric								
black-fabric								
black-obsidian								
black-oxidized-steel								
black-phenolic								
black-soft-plastic								

Material	Sample image	Near field 25° 1	Point sample 5	Sample image 1	Sample image 2	Near field 25° 2	Point sample 20	Reference
blue-acrylic								
blue-fabric								
blue-metallic-paint								
blue-metallic-paint2								
blue-rubber								
brass								
cherry-235								
chrome-steel								
chrome								
colonial-maple-223								

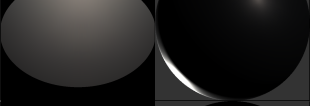
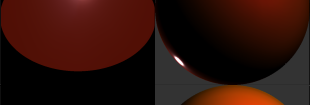
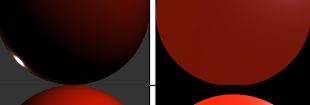
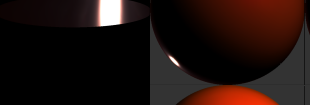
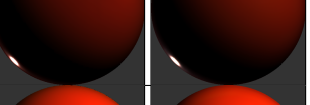
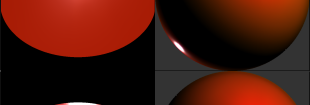
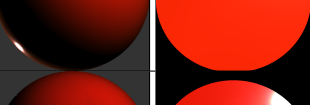
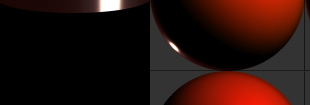
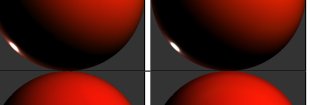
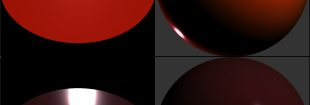
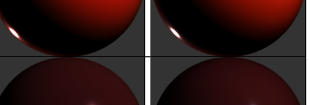
Material	Sample image	Near field 25° 1	Point sample 5	Sample image 1	Sample image 2	Near field 25° 2	Point sample 20	Reference
color-changing-paint1								
color-changing-paint2								
color-changing-paint3								
dark-blue-paint								
dark-red-paint								
dark-specular-fabric								
delrin								
fruitwood-241								
gold-metallic-paint								
gold-metallic-paint2								

Material	Sample image	Near field 25° 1	Point sample 5	Sample image 1	Sample image 2	Near field 25° 2	Point sample 20	Reference
gold-metallic-paint3								
gold-paint								
gray-plastic								
grease-covered-steel								
green-acrylic								
green-fabric								
green-latex								
green-metallic-paint								
green-metallic-paint2								
green-plastic								

Material	Sample image	Near field 25° 1	Point sample 5	Sample image 1	Sample image 2	Near field 25° 2	Point sample 20	Reference
hematite								
ipswich-pine-221								
light-brown-fabric								
light-red-paint								
maroon-plastic								
natural-209								
neoprene-rubber								
nickel								
nylon								
orange-paint								

Material	Sample image	Near field 25° 1	Point sample 5	Sample image 1	Sample image 2	Near field 25° 2	Point sample 20	Reference
pearl-paint								
pickled-oak-260								
pink-fabric								
pink-fabric2								
pink-felt								
pink-jasper								
pink-plastic								
polyethylene								
polyurethane-foam								
pure-rubber								

Material	Sample image	Near field 25° 1	Point sample 5	Sample image 1	Sample image 2	Near field 25° 2	Point sample 20	Reference
purple-paint								
pvc								
red-fabric								
red-fabric2								
red-metallic-paint								
red-phenolic								
red-plastic								
red-specular-plastic								
silicon-nitride								
silver-metallic-paint								

Material	Sample image	Near field 25° 1	Point sample 5	Sample image 1	Sample image 2	Near field 25° 2	Point sample 20	Reference
silver-metallic-paint2								
silver-paint								
special-walnut-224								
specular-black-phenolic								
specular-blue-phenolic								
specular-green-phenolic								
specular-maroon-phenolic								
specular-orange-phenolic								
specular-red-phenolic								
specular-violet-phenolic								

Material	Sample image	Near field 25° 1	Point sample 5	Sample image 1	Sample image 2	Near field 25° 2	Point sample 20	Reference
specular-white-phenolic								
specular-yellow-phenolic								
ss440								
steel								
teflon								
tungsten-carbide								
two-layer-gold								
two-layer-silver								
violet-acrylic								
violet-rubber								

Material	Sample image	Near field 25° 1	Point sample 5	Sample image 1	Sample image 2	Near field 25° 2	Point sample 20	Reference
white-acrylic								
white-diffuse-ball								
white-fabric								
white-fabric2								
white-marble								
white-paint								
yellow-matte-plastic								
yellow-paint								
yellow-phenolic								
yellow-plastic								